

Direct Spectroscopic Evidence for the Formation of One-Dimensional Wetting Wires During the Growth of InGaAs/GaAs Quantum Dot Chains

Xiaoyong Wang,^{*,†} Zhiming M. Wang,[‡] Baolai Liang,[‡] Gregory J. Salamo,[‡] and Chih-Kang Shih[†]

*Department of Physics, the University of Texas at Austin, Austin, Texas 78712, and
Department of Physics, University of Arkansas, Fayetteville, Arkansas 72701*

Received February 6, 2006; Revised Manuscript Received July 24, 2006

ABSTRACT

We report direct spectroscopic evidence for the formation of one-dimensional (1D) wetting wires (WWs) during the Stransky–Krastanov growth of InGaAs/GaAs quantum dot (QD) chains. The wire-like nature of these 1D WWs was demonstrated by their 1D density of states and absorption anisotropies from the photoluminescence excitation measurements. Two groups of QDs were found sitting on top of these 1D WWs and the traditional two-dimensional wetting layers, respectively, with size-dependent emission polarization anisotropies of ca. 6–25% because of their elongated shapes.

Zero-dimensional (0D) self-assembled quantum dots (QDs) have attracted more and more research efforts in recent years because of their atomic-like fundamental properties and practical applications in lasers, photodetectors, and quantum technology.¹ In a typical Stransky–Krastanov (S–K) growth of self-assembled QDs, the lattice mismatch strain provides a driving force for the transition from two-dimensional (2D) layer-by-layer to three-dimensional (3D) islanding growth mode after the critical layer thickness of a few monolayers (MLs) is exceeded.² For a long time, the resulting system has been described as a random distribution of 0D QDs lying above an ultrathin 2D wetting layer (WL) and no other intermediate growth modes have ever been observed beyond this 2D-to-3D mode transition scenario.

Only recently was it proposed that by appropriately controlling strain in the S–K growth of multilayer InGaAs/GaAs QDs another new growth mode could occur, leading to the formation of one-dimensional (1D) WLs (hereafter denoted by 1D wetting wires (WWs) because of their wire-like properties discussed later) on top of the traditional 2D WL and serving as bases for the formation of QD chains^{3–5} (see Figure 1a). Although the existence of such 1D WWs was suggested previously from the transmission electron microscopy (TEM) measurements and the temperature-dependent behaviors of carrier transfer among QDs,³ no direct

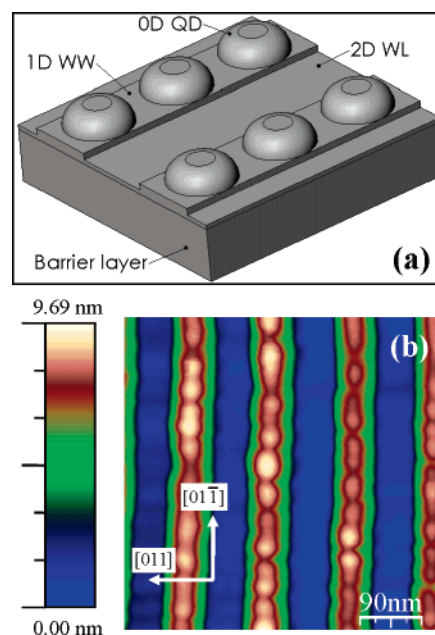


Figure 1. (a) Schematic diagram for the arrangement of 2D WL, 1D WWs, and 0D QDs in the InGaAs/GaAs QD chain sample. Only one layer of QDs was shown for simplicity. The dimension of each component was not drawn to scale. (b) $450 \times 450 \text{ nm}^2$ AFM image of the InGaAs/GaAs QD chains. Left: height scale bar of the AFM image.

* Corresponding author. E-mail: xywang@physics.utexas.edu.

[†] University of Texas at Austin.

[‡] University of Arkansas.

spectroscopic evidence has ever been provided. Moreover, if such novel quantum nanostructures of 1D WWs really

exist, then it is important to explore their fundamental optoelectronic properties for any future device applications.

In this letter, we provide *direct* spectroscopic evidence for the formation of 1D WWs during the S–K growth of InGaAs/GaAs QD chains from the photoluminescence (PL) and PL excitation (PLE) measurements. The wire-like nature of these 1D WWs was demonstrated by their 1D density of states (DOS) and the anisotropic absorption properties. Two groups of QDs were found sitting on top of these 1D WWs and the traditional 2D WLs, respectively, with size-dependent emission polarization anisotropies of ca. 6–25% because of their elongated shapes. The correlated relationship observed between smaller (larger) QDs and 1D WWs (2D WLs) suggests the occurrence of mass transfer between 1D WWs and 0D QDs in the formation process of QD chains.

The InGaAs/GaAs QD chains were grown by molecular beam epitaxy (MBE) using a procedure similar to that described in ref 4. After growing a 0.5 μm GaAs buffer layer on a semi-insulating GaAs (100) substrate at 580 $^{\circ}\text{C}$, the temperature was reduced to 540 $^{\circ}\text{C}$ for the subsequent growth of 17-period (67 MLs GaAs)/(12 MLs $\text{In}_{0.3}\text{Ga}_{0.7}\text{As}$) multi-layer structures. The last $\text{In}_{0.3}\text{Ga}_{0.7}\text{As}$ QD layer was deposited without a final GaAs capping layer for the purpose of atomic force microscopy (AFM) measurements. Long QD chains separated ~ 100 nm from each other can be seen clearly from the AFM image in Figure 1b. The QDs are slightly elongated along the chain direction of $[01\bar{1}]$, with the average diameter and height of ~ 45 nm and ~ 2 nm, respectively. Formation of these QD chains can be explained^{4,5} by the larger surface diffusion length of materials and, consequently, greater strain relaxation along $[01\bar{1}]$ than along $[011]$, caused mainly by the (2×4) surface reconstruction with dimmer rows running along $[01\bar{1}]$. When multiple layers of QDs are grown, this kind of elliptical strain relief can be sequentially transferred to the succeeding layers and eventually leads to the formation of QD chains with asymmetric separations between neighboring QDs along $[01\bar{1}]$ and $[011]$ directions.

The QD chain sample was mounted in a He flow cryostat and cooled to ~ 8 K for all the PL and PLE measurements using a pulsed Ti:Sapphire laser. The excitation laser beam was focused onto the sample surface at an incident angle of $\sim 45^{\circ}$ relative to the normal direction, while optical emissions from the sample were collected vertically by a microscope objective and sent through a 0.5 meter spectrometer to a charge coupled device (CCD) camera. PL spectra of the sample measured with laser power densities (I_{ex}) of P_0 , $10 P_0$, and $100 P_0$ are shown in Figure 2a, where P_0 was ~ 5 W/cm^2 and the excitation laser wavelength was ~ 780 nm. As verified by single QD spectroscopy and discussed later in the text, the two PL peaks centering around ~ 941 nm and ~ 970 nm originate from the optical emissions of 0D QDs. When I_{ex} was varied below ~ 5 W/cm^2 , there was nearly no change in the relative amplitudes of these two peaks, implying that they were from two groups of QDs with different average sizes. When I_{ex} was increased above ~ 5 W/cm^2 , the PL intensity of the higher-energy peak increased much faster than that of the lower-energy one, which saturated at ~ 200 W/cm^2 . It can also be seen from Figure

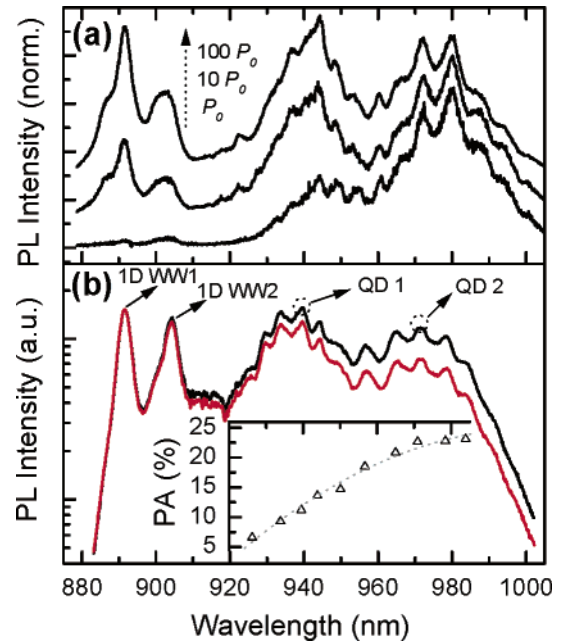


Figure 2. (a) PL spectra of the sample excited with three different laser power densities of P_0 , $10 P_0$, and $100 P_0$ (from bottom to top), respectively, where P_0 was ~ 5 W/cm^2 . (b) PL spectra of the sample detected for emitted light with polarizations parallel (black line) and perpendicular (red line) to the QD chain direction of $[01\bar{1}]$. The excitation laser power density was ~ 600 W/cm^2 . The black arrows marked the PL peak positions for two types of 1D WWs and QDs. Inset: polarization anisotropy (PA) of QDs measured at different emission wavelengths (the dotted line used here is just for guiding the eyes). In both a and b, the excitation laser wavelength was ~ 780 nm. The small quasi-periodic modulations of the PL spectra were caused by the Etalon effect of the detection CCD. The slightly different PL peak positions in a and b are due to the measurements performed at different sample positions and also the relatively higher laser power density used for the PL spectra in b.

2a that, with the increasing I_{ex} , two other well-defined peaks began to emerge around ~ 892 nm and ~ 904 nm, respectively, and are ascribed later in the text to be from the optical emissions of 1D WWs. Thus, the isolated emission peaks of 1D WWs from those of 0D QDs provide us with a unique opportunity to explore the opto-electronic properties of 1D WWs as well as their possible interactions with 0D QDs.

In Figure 2b, we show two PL spectra for emitted light with polarizations parallel (black line) and perpendicular (red line) to the QD chain direction of $[01\bar{1}]$, where I_{ex} was ~ 600 W/cm^2 and the excitation laser wavelength was ~ 780 nm. For convenience, the central positions of the four emission peaks mentioned above were marked by arrows to stand for two types of 1D WWs: “1D WW1” and “1D WW2”, and two types of QDs: “QD1” and “QD2”. It was found that optical emissions from all 0D QDs were preferentially polarized along the chain direction with the polarization anisotropy (PA)⁶ increasing from $\sim 6\%$ at shorter to $\sim 25\%$ at longer emission wavelengths (see the inset of Figure 2b). The larger value of emission PA for larger QDs (longer emission wavelengths) can be explained by their more anisotropic shapes and/or the size-dependent piezoelectric fields.^{3,7–9} Meanwhile, the emission PA of “1D WW2” was only $\sim 4\%$ and “1D WW1” exhibits nearly no polarization

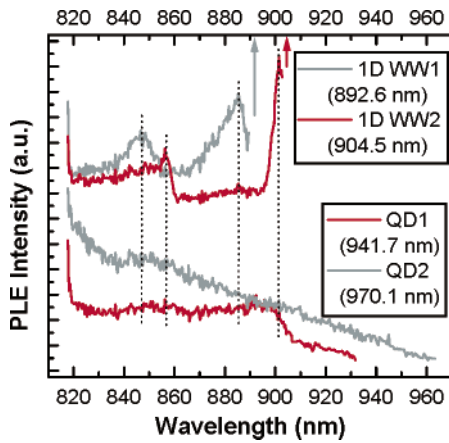


Figure 3. (Top) PLE spectra of “1D WW1” (gray line) and “1D WW2” (red line) monitored at 892.6 nm (marked by the gray arrow) and 904.5 nm (marked by the red arrow), respectively. (Bottom) PLE spectra of “QD1” (red line) and “QD2” (gray line) monitored at 941.7 and 970.1 nm, respectively. The PLE spectra of 1D WWs were offset relative to those of QDs for clarity. The polarization direction of the excitation laser was chosen to be parallel to the QD chain direction of [011] for the PLE measurements. The four vertical dotted lines are set at the PLE peaks of 1D WWs for guiding the eyes.

dependence in its optical emissions. The polarization measurements discussed here were calibrated carefully by using an isotropic white light source to avoid any detection artifacts due to the anisotropic response of the spectrometer.

To understand the opto-electronic properties of “1D WW1” and “1D WW2”, in Figure 3, we plot the PLE spectra detected at their respective PL peak positions. For self-assembled QD samples grown under S–K conditions, the DOS for 2D WL is universally described as decreasing continuously from the barrier energy gap toward lower energies, which should also be reflected in the PLE spectrum of 0D QDs formed on top of them.^{10,11} Thus, the higher- and lower-energy absorption subbands observed in the PLE spectra of both “1D WW1” and “1D WW2” unambiguously testify their structural origins from 1D WWs depicted in Figure 1a. For “1D WW1”, the FWHMs (full width at half-maximum)¹² of the higher- and lower-energy subbands are ~ 14.6 meV and ~ 10.3 meV, respectively, and the Stokes shift, defined as the energy difference between the peaks of the lower-energy PLE subband and the PL, is ~ 11.4 meV. For “1D WW2”, the Stokes shift is with a smaller value of ~ 4.6 meV so that the scanning of its PLE spectrum (from shorter to longer wavelengths) was stopped right after passing the peak of the lower-energy subband to avoid the scattering of excitation laser light. As a result, we can only estimate the FWHM for the higher-energy PLE subband of “1D WW2”, which is ~ 8.8 meV.

To gain further insight into the nature of these two absorption subbands of 1D WWs, we performed polarized PLE (namely, absorption PA) measurements. Figure 4a displays the PLE spectra of “1D WW1” excited with laser polarizations parallel and perpendicular to the QD chain direction of [011], respectively, and the absorption anisotropy can be seen clearly in both the lower- and higher-energy subbands. The same polarized PLE measurements were

performed on “1D WW2” and very similar results were obtained. In Figure 4b and c, we plot the excitation-polarization-angle dependent PL intensity traces for both “1D WW1” and “1D WW2” with the excitation laser wavelengths set at the peak positions of their respective lower- and higher-energy PLE subbands. The absorption PAs were calculated to be $\sim 7.5\%$ ($\sim 6.0\%$) and $\sim 10.0\%$ ($\sim 10.5\%$), respectively, for the lower- and higher-energy PLE subbands of “1D WW1” (“1D WW2”). For 2D quantum wells (QWs) fabricated on top of GaAs (100) substrates, it has been well-established that there should be no emission and absorption PAs^{13–15} and, thus, the absorption anisotropy demonstrated from Figure 4 for the two types of 1D WWs strongly confirms their 1D nature of quantum confinement. As seen from Figure 4a, except for the intensity difference, the two polarized PLE spectra show similar spectral profiles. Moreover, in Figure 4b and c, the excitation-polarization-angle dependent PL intensity traces for the lower- and higher-energy PLE subbands of “1D WW1”/“1D WW2” are in phase, so both of them should result from the heavy hole to conduction band transitions.^{16,17} The energy levels of light holes could be decoupled and shifted far away from those of heavy holes possibly due to the strain effects.^{16,17}

We should note here that the smaller PA in emission (see Figure 2b) relative to that in absorption may not be an intrinsic property of these 1D WWs because both the emission and absorption processes should be governed by the same transition matrix elements. Because the formation of 1D quantum wires (QWRs) with higher structural quality is normally associated with a smaller Stokes shift,¹⁷ the larger Stokes shift of “1D WW1” relative to that of “1D WW2” implies that it should be accompanied with more defects in the formation process. We thus tentatively attribute the reduction of emission PA, especially in “1D WW1”, to the localization of excitons at the defect centers with isotropic emission properties.^{13,14,16}

Besides the polarized PLE measurements that have revealed the 1D wire-like nature of “1D WW1” and “1D WW2”, more quantum confinement information can be obtained by looking at the wavelength-dependent behaviors of their respective PLE spectra in Figure 3. For “1D WW1”, when moving from long to short wavelengths, the PLE signal of the lower-energy absorption subband increases sharply to a maximum and then decreases slowly to a minimum, so does the higher-energy subband that decreases back to the *same* amplitude level. These behaviors represent very well the 1D DOS expected from QWRs.¹⁸ For “1D WW2”, with decreasing wavelength, the higher-energy PLE subband decreases to a *higher* signal level than that of the lower-energy one, which is reminiscent of the 2D DOS of QWs including the excitonic effect.¹⁹ This kind of staircase-like PLE spectrum deviates from the 1D DOS and implies that “1D WW2” may still keep some QW-like properties because of the relatively large width of ~ 45 nm of these 1D WWs.

In Figure 3, we also plot the PLE spectra measured for both “QD1” and “QD2” at their respective PL peak positions (marked by the dotted circles in Figure 2b). It can be seen that the PLE spectrum of “QD2” is dominated by a

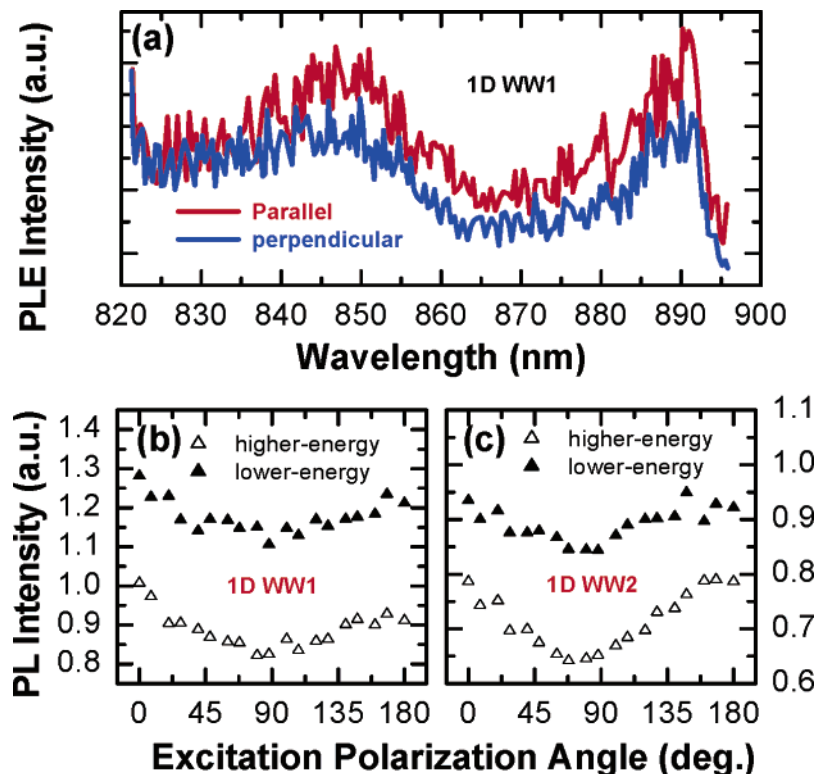


Figure 4. (a) PLE spectra of “1D WW1” measured with the excitation laser polarizations parallel (red line) and perpendicular (blue line) to the QD chain direction of $[01\bar{1}]$. (b and c) PL intensity traces of “1D WW1”/“1D WW2” as functions of excitation polarization angles. For “1D WW1”/“1D WW2” in b and c, the excitation laser wavelengths were 888 nm/900 nm and 847 nm/856 nm at the peaks of the lower-energy (\blacktriangle) and higher-energy (\triangle) PLE subbands, respectively. The direction of QD chains was set parallel to the 0° polarization direction of the excitation laser. The two sets of PL intensity traces for “1D WW1”/“1D WW2” in b and c were offset for clarity.

continuum-like feature generally observed in the PLE spectrum of 0D QDs formed directly on top of 2D WL.^{10,11} In contrast, the DOS discussed above for 1D WWs is dominant in the PLE spectrum of “QD1”, whose amplitude drops abruptly right after passing the energy gap of GaAs (~ 820 nm) and then evolves with increasing wavelengths to yield two absorption subbands. The 2D continuum is now only obvious at the long wavelength side from ~ 910 – 930 nm and possibly serving as a background for the other wavelength range from ~ 820 – 910 nm in the PLE spectrum of “QD1”. Thus, we can conclude that QDs in the ensemble of “QD2” with larger sizes are formed mainly on top of 2D WLs so that they possess similar absorption properties. Under similar arguments, QDs in the ensemble of “QD1” with smaller sizes are formed mainly on top of 1D WWs, which are likewise lying above 2D WLs (see Figure 1a).

During a traditional 2D-to-3D mode transition process under S–K conditions, the formation of 0D QDs will always induce a local depletion of the underlying 2D WL.¹¹ This gives us some clues to qualitatively explain the correlated relationship between “QD1” (“QD2”) and 1D WWs (2D WLs) by a mass transfer mechanism where the formation of 1D WWs causes the reduced materials and, consequently, reduced sizes of QDs on top of them. This mechanism is consistent with previous observations from structural studies^{3–5} of InGaAs/GaAs QD chains indicating that QDs with relatively larger sizes (“QD2”) are randomly distributed on top of 2D WL in the first layer. When more and more layers

are stacked, the chain-like structures begin to emerge and eventually evolve into fully developed QD chains at the top layers with relatively smaller sized QDs (“QD1”).

It can also be seen from the PLE spectrum of “QD2” in Figure 3 that, besides the dominant 2D WL feature, a weak peak can be resolved roughly at the energy position of the higher-energy PLE subband of “1D WW1”. This suggests that “1D WW1” should correspond to thinner 1D WWs connected with a small portion of the larger sized QDs in the ensemble of “QD2” at the bottom layers of the sample. Because the QD chains are still at the development stage in these layers, relatively larger thickness fluctuations of 1D WWs and more defect sites at their interfaces with 2D WLs and 0D QDs are expected. This is consistent with the relatively broader PLE subbands, larger Stokes shift, and smaller emission PA of “1D WW1” described earlier in the text. Also in Figure 3, the lower-energy PLE subband of “QD1” lies between those of “1D WW1” and “1D WW2”, whereas the higher-energy one occurs roughly at the same energy position as that of “1D WW2”. Moreover, the staircase-like feature observed in the PLE spectrum of “1D WW2” is more or less present in the PLE spectrum of “QD1”. All of these facts imply that the smaller-sized QDs in the ensemble of “QD1” are sitting mainly on top of thicker 1D WWs of “1D WW2” at the top layers of the sample with fully developed QD chains.

It should be mentioned that the PLE spectrum of “1D WW1” (“1D WW2”) was also detected at wavelengths in

its PL spectrum other than the one shown in Figure 3. The higher- and lower-energy PLE subbands can always be resolved and shift gradually to the red side with the increasing detection wavelength in each PL spectrum. However, when changing the detection wavelength in the PL spectrum from the long-wavelength edge of “1D WW1” to the short-wavelength edge of “1D WW2”, there is a sudden decrease in the peak energies of these two PLE subbands. As discussed earlier in the text, the thickness difference between “1D WW1” and “1D WW2” has already been established from their correlations with the larger- and smaller-sized QDs at the bottom and top layers of the sample. When assuming that the lateral width of these 1D WWs is close to the diameter of QDs on top of them (~ 45 nm), the quantization effect in the plane can be neglected and it is mainly the bimodal thickness distribution of 1D WWs that gives rise to the step changes between both the PL and PLE peaks of “1D WW1” and “1D WW2”, although the compositional variations of In concentration may also play a role here.²⁰

The bimodal thickness (size) distribution of 1D WWs (QDs) implies that the development of QD chains in this sample is not a smooth process so that a transition stage may exist with a drastic increase of the 1D WW thickness and the associated decrease of QD size. Further optical investigations of more QD chain samples fabricated with controlled material transport by playing with growth interruptions^{4,5} may help to understand this transition stage. Also, to fully understand the electron and hole natures of the two PLE subbands, especially the appearance of QW-like feature in the PLE spectrum of “1D WW2”, complicated theoretical calculations are needed to consider the strain effect, the geometry of the 1D WWs, and the shape of the confining potentials influenced by both thickness and compositional changes.

In conclusion, we have provided direct spectroscopic evidence for the formation of 1D WWs during the S–K growth of InGaAs/GaAs QD chains. Our observations have led to a better understanding of the previously unexplored 2D-(1D WW)-3D mode transition process during the S–K growth of self-assembled QDs. We believe that these novel quantum nanostructures of QD chains, combining the multidimensional quantum confinements of 2D WL, 1D WWs, and 0D QDs will stimulate more theoretical interest in their fundamental opto-electronic properties. As revealed from our preliminary studies,⁴ this new growth mode could be tailored by varying the In composition and barrier thickness to yield QDs and 1D WWs with expected sizes and thicknesses and, consequently, expected energy separations between their energy levels. This may render us the ability to effectively control the carrier transfer among QDs on top of 1D WWs for the quantum technology applications that require quantum information transfer between quantum

bits in different nanostructures of controlled positioning. The 1D WW subbands added to the absorption spectrum of 0D QDs as well as their size-dependent anisotropic optical emissions also make these InGaAs/GaAs QD chain structures promising in device applications of polarization-sensitive detectors and polarization-controlled surface-emitting lasers.^{7–9}

Acknowledgment. We gratefully acknowledge support of this work by NSF (DMR-0210383 and DMR-0306239), Office of Naval Research (N0014-04-1-033), Texas Advanced Technology program, and the W. M. Keck Foundation.

References

- (1) Petroff, P. M.; Lorke, A.; Imamoglu, A. *Phys. Today* **2001**, *54*, 46.
- (2) Heitz, R.; Ramachandran, T. R.; Kalburge, A.; Xie, Q.; Mukhametzhanov, I.; Chen, P.; Madhukar, A. *Phys. Rev. Lett.* **1997**, *78*, 4071.
- (3) Mazur, Yu. I.; Ma, W. Q.; Wang, X.; Wang, Z. M.; Salamo, G. J.; Xiao, M.; Mishima, T. D.; Johnson, M. B. *Appl. Phys. Lett.* **2003**, *83*, 987.
- (4) Wang, Zh. M.; Mazur, Yu. I.; Holmes, K.; Salamo, G. J. *J. Vac. Sci. Technol., B* **2005**, *23*, 1732.
- (5) (a) Schmidbauer, M.; Seydmohamadi, Sh.; Grigoriev, D.; Wang, Zh. M.; Mazur, Yu. I.; Schäfer, P.; Hanke, M.; Köhler, R.; Salamo, G. J. *Phys. Rev. Lett.* **2006**, *96*, 066108. (b) Wang, Z. M.; Holmes, K.; Mazur, Yu. I.; Salamo, G. J. *Appl. Phys. Lett.* **2004**, *84*, 1931.
- (6) The emission polarization anisotropy (PA) is defined as $(I_{\parallel} - I_{\perp})/(I_{\parallel} + I_{\perp})$, where I_{\parallel} and I_{\perp} are the PL intensities of emitted light with polarizations parallel and perpendicular to the QD chain direction. The absorption PA can be similarly defined.
- (7) Saito, H.; Nishi, K.; Sugou, S.; Sugimoto, Y. *Appl. Phys. Lett.* **1997**, *71*, 590.
- (8) Yu, P.; Langbein, W.; Leosson, K.; Hvam, J. M.; Ledentsov, N. N.; Bimberg, D.; Ustinov, V. M.; Egorov, A. Yu.; Zhukov, A. E.; Tsatsul'nikov, A. F.; Musikhin, Yu. G. *Phys. Rev. B* **1999**, *60*, 680.
- (9) Henini, M.; Sanguinetti, S.; Fortina, S. C.; Grilli, E.; Guzzi, M.; Panzarini, G.; Andreani, L. C.; Upward, M. D.; Moriarty, P.; Beton, P. H.; Eaves, L. *Phys. Rev. B* **1998**, *57*, R6815.
- (10) Toda, Y.; Moriwaki, O.; Nishioka, M.; Arakawa, Y. *Phys. Rev. Lett.* **1999**, *82*, 4114.
- (11) Kammerer, C.; Cassabo, G.; Voisin, C.; Delalande, C.; Roussignol, Ph.; Gerard, J. M. *Phys. Rev. Lett.* **2001**, *87*, 207401.
- (12) For convenience, we evaluate the FWHM of each asymmetric PLE subband only from its long-wavelength side, the broadening of which should result from the thickness/compositional fluctuations of 1D WWs.
- (13) Vouilloz, F.; Oberli, D. Y.; Dupertuis, M.-A.; Gustafsson, A.; Reinhardt, F.; Kapon, E. *Phys. Rev. Lett.* **1997**, *78*, 1580.
- (14) Santos, Paulo V.; Nötzel, R.; Ploog, K. H. *J. Appl. Phys.* **1999**, *85*, 8228.
- (15) Gershoni, D.; Brener, I.; Baraff, G. A.; Chu, S. N. G.; Pfeiffer, L. N.; West, K. *Phys. Rev. B* **1991**, *44*, 1930.
- (16) Martinet, E.; Dupertuis, M.-A.; Reinhardt, F.; Biasiol, G.; Kapon, E.; Stier, O.; Grundmann, M.; Bimberg, D. *Phys. Rev. B* **2000**, *61*, 4488.
- (17) Tsurumachi, N.; Son, C.-S.; Kim, T. G.; Takasuka, Y.; Ogura, M. *Jpn. J. Appl. Phys.* **2002**, *41*, 2679.
- (18) Jacak, L.; Hawrylak, P.; Wójs, A. *Quantum Dots*; Springer-Verlag: Berlin, 1998; p 15.
- (19) Dingle, R.; Wiegmann, W.; Henry, C. H. *Phys. Rev. Lett.* **1974**, *33*, 827.
- (20) Muraki, K.; Fukatsu, S.; Shiraki, Y.; Ito, R. *Appl. Phys. Lett.* **1992**, *61*, 557.

NL060271T